Diabetologia (2011) 54:2660–2668
DOI 10.1007/s00125-011-2248-8

ARTICLE

Critical role of chemokine (C-C motif) receptor 2 (CCR2) in the KK*Ay*$^{+}$*Apoe*$^{-/-}$ mouse model of the metabolic syndrome

H. G. Martinez · M. P. Quinones · F. Jimenez · C. A. Estrada · K. Clark · G. Muscogiuri · G. Sorice · N. Musi · R. L. Reddick · S. S. Ahuja

Received: 31 May 2011 / Accepted: 3 June 2011 / Published online: 21 July 2011

Abstract
Aims/hypothesis Chemokines and their receptors such as chemokine (C-C motif) receptor 2 (CCR2) may contribute to the pathogenesis of the metabolic syndrome via their effects on inflammatory monocytes. Increased accumulation of CCR2-driven inflammatory monocytes in epididymal fat pads is thought to favour the development of insulin resistance. Ultimately, the resulting hyperglycaemia and dyslipidaemia contribute to development of the metabolic syndrome complications such as cardiovascular disease and diabetic nephropathy. Our goal was to elucidate the role of CCR2 and inflammatory monocytes in a mouse model that resembles the human metabolic syndrome.
Methods We generated a model of the metabolic syndrome by backcrossing KK*Ay*$^{+}$ with *Apoe*$^{-/-}$ mice (KK*Ay*$^{+}$*Apoe*$^{-/-}$) and studied the role of CCR2 in this model system.
Results KK*Ay*$^{+}$*Apoe*$^{-/-}$ mice were characterised by the presence of obesity, insulin resistance, dyslipidaemia and increased systemic inflammation. This model also manifested two complications of the metabolic syndrome: atherosclerosis and diabetic nephropathy. Inactivation of *Ccr2* in KK*Ay*$^{+}$*Apoe*$^{-/-}$ mice protected against the metabolic syndrome, as well as atherosclerosis and diabetic nephropathy. This protective phenotype was associated with a reduced number of inflammatory monocytes in the liver and muscle, but not in the epididymal fat pads; circulating levels of adipokines such as leptin, resistin and adiponectin were also not reduced. Interestingly, the proportion of inflammatory monocytes in the liver, pancreas and muscle, but not in the epididymal fat pads, correlated significantly with peripheral glucose levels.
Conclusions/interpretation CCR2-driven inflammatory monocyte accumulation in the liver and muscle may be a critical pathogenic factor in the development of the metabolic syndrome.

Keywords Animal-mouse · Basic science · Cardiac complications · Experimental immunology · KO mice · Metabolic syndrome · Nephropathy

Abbreviations

CCL2	Chemokine (C-C motif) ligand 2
CCR2	Chemokine (C-C motif) receptor 2
GSK-3β	Glycogen synthase kinase 3β
GTT	Glucose tolerance test
HFD	High-fat diet

H. G. Martinez and M. P. Quinones contributed equally to this study.

Electronic supplementary material The online version of this article (doi:10.1007/s00125-011-2248-8) contains peer-reviewed but unedited supplementary material, which is available to authorised users.

H. G. Martinez · F. Jimenez · S. S. Ahuja
South Texas Veterans Health Care System,
Audie L. Murphy Division,
San Antonio, TX, USA

H. G. Martinez · F. Jimenez · C. A. Estrada · K. Clark · G. Muscogiuri · G. Sorice · N. Musi · S. S. Ahuja (✉)
Department of Medicine (MC 7870),
University of Texas Health Science Center at San Antonio,
7703 Floyd Curl Drive,
San Antonio, TX 78229-3900, USA
e-mail: ahuja@uthscsa.edu

M. P. Quinones
Department of Psychiatry, University of Texas Health Science Center at San Antonio (UTHSCSA),
San Antonio, TX, USA

R. L. Reddick
Department of Pathology, University of Texas Health Science Center at San Antonio (UTHSCSA),
San Antonio, TX, USA

ITT	Insulin tolerance test
LPS	Lipopolysaccharide
pGSK-3β	Phosphorylation of GSK-3β
STAT3	Signal transducer and activator of transcription 3

Introduction

The metabolic syndrome, a condition that affects 47 million Americans [1], clinically manifests as insulin resistance, atherogenic dyslipidaemia (high triacylglycerol, hypercholesterolaemia with low HDL-cholesterol and/or high LDL-cholesterol), hypertension, obesity and increased systemic inflammation. Complications of the metabolic syndrome include coronary artery disease [2] caused by worsening of atherosclerosis, and diabetic nephropathy [3], the most common cause of end-stage renal disease worldwide [4].

Systemic inflammation as well as local effects of inflammatory cells are thought to play an important role in the development of processes related to the metabolic syndrome, such as insulin resistance and atherogenesis [5]. Chemokines and their receptors are vital to the recruitment of leucocytes and many other inflammatory processes [6]. For example, chemokine (C-C motif) receptor 2 (CCR2) is indispensable for adequate monocyte/macrophage trafficking and activation [7, 8]. This role of CCR2 may be important in the emergence of the metabolic syndrome, as indicated by the finding that mice in which CCR2 is genetically ablated or pharmacologically blocked were protected against development of insulin resistance and obesity, presumably by decreasing monocyte infiltration into fat [9, 10]. Insights derived from other rodent models also suggest that defective macrophage migration induced by modulating the CCR2 ligand, chemokine (C-C motif) ligand 2 (CCL2, also known as MCP-1), may influence atherosclerosis [11] and diabetic nephropathy [12]. However, no single current animal model captures the complex phenotype seen in humans with the metabolic syndrome (Electronic supplementary material [ESM] Table 1).

We therefore generated a murine model of the metabolic syndrome by backcrossing KKAy^{+} mice (a polygenic model of type 2 diabetes [13]) with atherosclerosis-prone $Apoe^{-/-}$ mice [14]. KK$Ay^{+}Apoe^{-/-}$ mice progressively developed obesity, insulin resistance, dyslipidaemia and complications of the metabolic syndrome such as atherosclerosis and diabetic nephropathy. We also found that *Ccr2* inactivation in KK$Ay^{+}Apoe^{-/-}$ mice protected against the metabolic syndrome-defining features and complications. Interestingly, after excluding several confounding factors, we found that the protective effect of *Ccr2* ablation is possibly linked to reduced accumulation of inflammatory monocytes in the muscle and liver, but not in the epididymal fat pads.

Methods

Mice, diet and induction of chronic inflammation

KKAy^{+} mice (stock KK-Ay/TaJcl) were purchased from CLEA Japan (Tokyo, Japan). KKAy^{+} mice were crossed with $Apoe^{-/-}$ mice for two to three generations until a sufficient number of mice with the genotype KK$Ay^{-}Apoe^{-/-}$ or KK$Ay^{+}Apoe^{-/-}$ were obtained. KK$Ay^{-}Apoe^{-/-}$ or KK$Ay^{+}Apoe^{-/-}$ mice were further bred with $Apoe^{-/-}Ccr2^{-/-}$ mice (C57BL/6J background). Our laboratory and others have described the generation and backcrossing procedures of the later two strains [15–17]. The resulting intercross mating produced the experimental animal groups. *Ccr2* and *Apoe* genotypes were confirmed by PCR, as previously described [15]. Visual inspection of the coat colour further verified the *Ay* (agouti) allele transmission, with yellow coat identifying positive (Ay^{+}) transmission, whereas black coat indicated negative (Ay^{-}) allele transmission. KK$Ay^{-}Apoe^{-/-}$ and KK$Ay^{-}Apoe^{-/-}Ccr2^{-/-}$ littermates served as controls for all Ay^{+} mice.

All data sets presented here were derived from mice at 25±5 weeks of age. All animals were kept under pathogen-free conditions and the Institutional Animal Care and Use Committee of the University of Texas Health Science Center at San Antonio (UTHSCSA) approved all protocols.

Mice genotype, dual energy X-ray absorptiometry (DEXA) scan, stains in kidneys, blood pressure analysis, electron microscopy, Akt phospho 7-plex panel and Ingenuity pathway analysis are described in more detail in the ESM Methods.

Weight analyses and food intake

Mice were followed for 8 to 10 weeks, fed with a normal diet and had body weights recorded weekly by an investigator blind to the experimental groups. A second experimental set of animals was individually housed in metabolism cages for 3 to 4 days for acclimatisation, after which food and water intake was recorded every 24 h for four consecutive days.

Metabolic variables

Blood samples were obtained to determine glucose levels using a glucose monitor (Ascencia Elite; Bayer, Mishawaka, IN, USA) and cholesterol levels (Vetometer II; Kacey, Asheville, NC, USA). Serum ELISA (performed following manufacturers' instructions) was done to measure levels of insulin (Crystal Chem, Downers Grove, IL, USA), TNFα and IL-6 (eBiosciences, San Diego, CA, USA), and leptin, resistin and adiponectin (Alpha Diagnostics, San Antonio, TX, USA) in sera. Triacylglycerol levels were

assessed with a Trace Infinity reagent (Thermo Scientific, Waltham, MA, USA). For details on insulin tolerance test (ITT) and glucose tolerance test (GTT), see ESM Methods.

Serum creatinine was measured using HPLC. Briefly, 1 ml acetonitrile was added to 10 μl serum, incubated for 20 min, mixed and centrifuged for 15 min at 16,400 *g* after which the sample was concentrated by speed vac. Before use, the sample was re-suspended with 120 μl of the mobile phase (5 mmol/l sodium acetate pH 5.1) and 25 μl was injected into the machine.

Urine albumin and creatinine collected in metabolism cages were analysed by ELISA (Exowell, Philadelphia, PA, USA), following the manufacturer's protocol.

Immunohistochemistry and histomorphometric analysis

Sections of atherosclerotic plaques were stained with the ER-HR3 marker for macrophages, as previously described [18]. For macrophage staining in liver, F4/80 antibody was used (clone A1-3; AbD Serotec, Raleigh, NC, USA). Percentage of stained area was determined using ImageJ software (National Institutes of Health, Bethesda, MD, USA).

Histomorphometric analysis of atherosclerotic plaques at the level of the aortic root was performed as previously described [18]. For the histomorphometric analysis of the kidneys, glomerular volume was calculated according to the formula: $GV=(\beta/\kappa) \times (GA)^{3/2}$, where GV is glomerular volume, $\beta=1.38$, $\kappa=1.1$ and GA is glomerular area, as described by Pagtalunan et al. [19].

Flow cytometry

Mice were perfused with 15 ml cold PBS prior to organ removal and single cell suspensions were prepared as described by Soos et al. [20]. Cell suspensions were stained with diverse combinations of antibodies including CD11b APC, Ly6C FITC and Ly6G PE or isotype-matched antibodies (BD Biosciences, San Jose, CA, USA), and analysed on a FACScalibur with Cell Quest software (BD Biosciences).

Statistical analysis

For brevity, data presented compare KK*Ay*$^{+}$*Apoe*$^{-/-}$ and KK*Ay*$^{+}$*Apoe*$^{-/-}$*Ccr2*$^{-/-}$ mice. However all experimental groups were included as controls in each experiment. Data represent the mean±SD; statistical analysis was performed with Stata (StataCorp, College Station, TX, USA) or SPSS (Chicago, IL, USA) statistical software. Based on the number of groups and their distribution (normally distributed or not), non-paired *t* test, one-way ANOVA, Kruskal–Wallis, Mann–Whitney or Fisher's exact tests were performed. Statistical significance was accepted at $p<0.05$.

Results

Murine model of the metabolic syndrome

Weight gain KK*Ay*$^{+}$*Apoe*$^{-/-}$ and KK*Ay*$^{+}$*Apoe*$^{-/-}$*Ccr2*$^{-/-}$ mice, and their respective controls (KK*Ay*$^{-}$*Apoe*$^{-/-}$ and KK*Ay*$^{-}$*Apoe*$^{-/-}$*Ccr2*$^{-/-}$ littermates) were followed for up to 10 weeks, during which weight and food intake were assessed. Weight in KK*Ay*$^{+}$*Apoe*$^{-/-}$ mice increased over time and was significantly higher than in controls (Table 1, ESM Fig. 1a). Notably, *Ccr2* inactivation in KK*Ay*$^{+}$*Apoe*$^{-/-}$ mice significantly ameliorated the total weight gained after 10 weeks of follow-up (Table 1, ESM Fig. 1a). Comparable food intake in KK*Ay*$^{+}$*Apoe*$^{-/-}$and KK*Ay*$^{+}$*Apoe*$^{-/-}$*Ccr2*$^{-/-}$ mice suggested that mechanisms other than energy intake accounted for weight differences (Fig. 1b).

Glucose and insulin resistance Inactivation of *Ccr2* in KK*Ay*$^{+}$*Apoe*$^{-/-}$ mice blunted the development of hyperglycaemia and hyperinsulinaemia that were observed at 10 weeks of follow-up (Table 1). Furthermore, using the HOMA of insulin resistance, we found that inactivation of *Ccr2* protected against insulin resistance in KK*Ay*$^{+}$*Apoe*$^{-/-}$ mice. This notion was substantiated further by results from ITT (Fig. 1c) and GTT (Fig. 1d).

Differences in fasting glucose between KK*Ay*$^{+}$*Apoe*$^{-/-}$ (n=10) and *Ccr2*$^{-/-}$ (n=8) mice remained significant even after accounting for the weight differences. A multivariate analysis that included age, sex and weight as covariates revealed that *Ccr2* inactivation was associated with significantly lower levels of glucose in KK*Ay*$^{+}$*Apoe*$^{-/-}$ mice (8.1±0.6 vs 7.0±0.6 mmol/l for KK*Ay*$^{+}$*Apoe*$^{-/-}$ vs KK*Ay*$^{+}$*Apoe*$^{-/-}$*Ccr2*$^{-/-}$, p=0.002; data not shown).

Table 1 Metabolic variables

Variable	KK*Ay*$^{+}$*Apoe*$^{-/-}$		*p* value
	Ccr2$^{+/+}$	*Ccr2*$^{-/-}$	
Body weight (g)	45.0±6.0	29.0±5.0	0.01
Weight, epididymal fat pads (g)	2.5±0.6	1.9±0.5	0.21
Glucose (mmol/l)	13.5±7.5	10.6±4.5	0.01
Insulin (pmol/l)	219.2±4.0	151.5±4.0	0.03
HOMA-IR	19.0±0.2	10.3±0.1	0.04
Cholesterol (mmol/l)	7.6±0.6	7.5±0.5	0.92
Triacylglycerol (mmol/l)	1.3±0.2	1.3±0.3	0.90

Values are mean ± SD

Mice were 20±5 weeks of age; each group contained n=3–5 mice (one representative experiment of three performed is shown)

HOMA-IR, HOMA of insulin resistance (determined using a web calculator found at www.hepcnomads.co.uk/HOMACalc.htm)

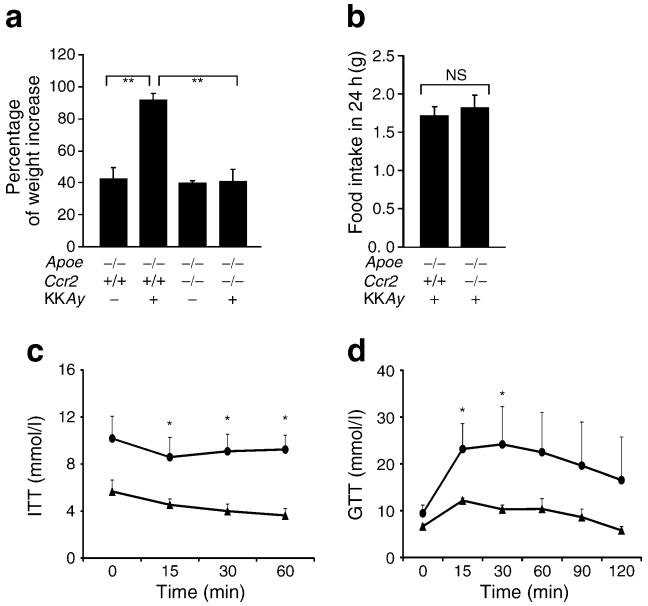

Fig. 1 Weight and glucose analysis. **a** Percentage of weight increase was determined by comparing the mean weight in each group, following the mice from week 10 to 18. *Ccr2* inactivation in the pathogenic KK*Ay*$^{+}$*Apoe*$^{-/-}$ mice led to a significant reduction in the percentage of weight gain. **b** Food intake during 24 h periods was quantified for four consecutive days; no difference was seen between KK*Ay*$^{+}$*Apoe*$^{-/-}$ and KK*Ay*$^{+}$*Apoe*$^{-/-}$*Ccr2*$^{-/-}$ mice. **a**, **b** Data are representative of experiments performed three times; n=3–5. Significant decrease in ITT (**c**) and GTT (**d**) values for KK*Ay*$^{+}$*Apoe*$^{-/-}$*Ccr2*$^{-/-}$ mice (black triangles) compared with KK*Ay*$^{+}$*Apoe*$^{-/-}$ mice (black circles) at 12 weeks of age; n=3–5 per group. *p<0.05 vs KK*Ay*$^{+}$*Apoe*$^{-/-}$*Ccr2*$^{-/-}$ value at the same time point; **p<0.001

Dyslipidaemia While genetic inactivation of *Apoe* is associated with significantly higher total cholesterol levels but normal triacylglycerol [14], the *Ay*$^{+}$ phenotype is associated with hypertriacylglycerolaemia [21, 22]. Consistent with this notion, we found that KK*Ay*$^{+}$*Apoe*$^{-/-}$ mice displayed hypercholesterolaemia and hypertriacylglycerolaemia compared with KK*Ay*$^{-}$*Apoe*$^{-/-}$ mice (data not shown). *Ccr2* inactivation did not affect triacylglycerol or cholesterol levels, as they were comparable between KK*Ay*$^{+}$*Apoe*$^{-/-}$ and KK*Ay*$^{+}$*Apoe*$^{-/-}$*Ccr2*$^{-/-}$ mouse groups (Table 1).

Blood pressure Previous reports had suggested that KK*Ay*$^{+}$ mice had higher blood pressure than C57BL/6J controls [23, 24]. However, we found that KK*Ay*$^{+}$ and KK*Ay*$^{-}$*Apoe*$^{-/-}$ mice had comparable blood pressure (data not shown). There were no differences in blood pressure between KK*Ay*$^{+}$*Apoe*$^{-/-}$ and KK*Ay*$^{+}$*Apoe*$^{-/-}$*Ccr2*$^{-/-}$ mice (ESM Fig. 1b).

Systemic inflammation In humans, pro-inflammatory cytokines such as IL-6 and TNFα have been extensively associated with the metabolic syndrome [25]. However, we did not find any differences in circulating TNFα and IL-6 levels between KK*Ay*$^{+}$*Apoe*$^{-/-}$ and KK*Ay*$^{-}$*Apoe*$^{-/-}$ mice (data not shown). We also tested a different source of inflammation such as the amount of circulating adipokines, and we found significantly low adiponectin and high leptin levels in KK*Ay*$^{+}$*Apoe*$^{-/-}$ mice compared with C57BL/6 controls (data not shown). However, there were no differences in circulating levels of adiponectin, leptin or resistin between KK*Ay*$^{+}$*Apoe* $^{-/-}$ and KK*Ay*$^{+}$*Apoe*$^{-/-}$*Ccr2*$^{-/-}$ mice, including KK*Ay*$^{-}$ mice as a control (ESM Table 2). Therefore, we tested other potential indicators of inflammation such as the proportion of inflammatory monocytes in blood. We found a significant increase in the proportion of inflammatory monocytes in KK*Ay*$^{+}$*Apoe*$^{-/-}$ mice compared with KK*Ay*$^{+}$*Apoe*$^{-/-}$ *Ccr2*$^{-/-}$ mice (Table 2).

Complications of the metabolic syndrome in our murine model

Cardiovascular disease The metabolic syndrome is a major risk factor for the development of atherosclerosis with high overall mortality; this risk factor applies independently of diabetes mellitus [26]. We observed that KK*Ay*$^{+}$ mice (with intact *Apoe* gene) did not develop atherosclerotic plaques even when on a high-fat diet (HFD) or under chronic inflammation induced by weekly lipopolysaccharide (LPS) injections (ESM Fig. 1c). We then asked whether the metabolic syndrome state in KK*Ay*$^{+}$*Apoe*$^{-/-}$ mice could worsen the atherosclerotic phenotype of *Apoe*$^{-/-}$ mice. We found that KK*Ay*$^{+}$*Apoe*$^{-/-}$ mice developed significantly larger atherosclerotic plaques than KK*Ay*$^{-}$*Apoe*$^{-/-}$ mice (Fig. 2a, b). These plaques also contained significantly higher proportion of macrophage infiltration (Fig. 2c, d). Furthermore, the protection against the metabolic syndrome that is afforded by the *Ccr2*-null state in KK*Ay*$^{+}$*Apoe*$^{-/-}$ mice was associated with a significant reduction in atherosclerotic plaque burden (Fig. 2a, b) and macrophage density (Fig. 2c, d).

Table 2 Effect of *Ccr2* inactivation on the proportion of inflammatory monocytes in different organs

Organ	KK*Ay*$^{+}$*Apoe*$^{-/-}$		Statistics	
	Ccr2$^{+/+}$	*Ccr2*$^{-/-}$	p value	df
Liver	7.3±0.5	1.6±0.4	0.001	24.2
Epididymal fat pads	4.6±0.9	4.2±0.8	NS	–
Pancreas	3.3±1.1	2.5±1.1	NS	–
Muscle	24.4±3.0	19.3±2.5	0.0001	9.7
Blood	10.7±0.5	1.1±0.3	0.0001	84.7

Values are mean ± SE; n=9–15; df=4; partial correlation accounting for age, sex and body weight

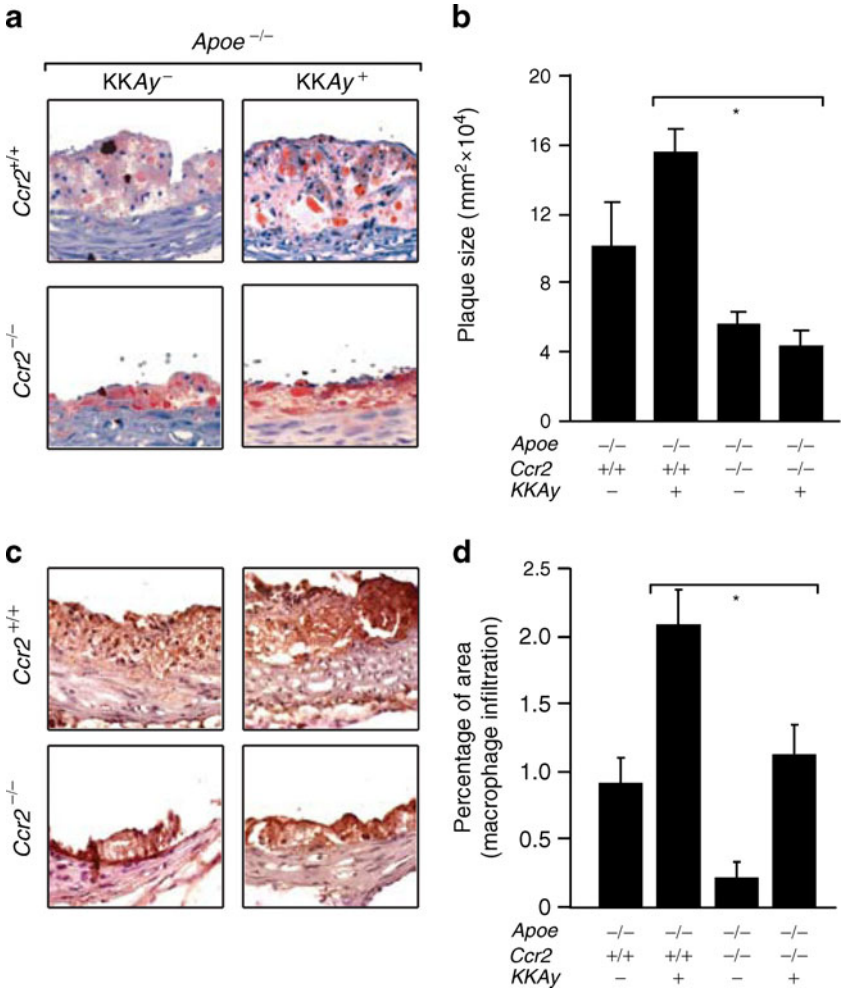

Fig. 2 Effects of *Ccr2*-null state on the development of atherosclerosis in the metabolic syndrome. **a** Representative images of aortic plaque size; tissue was stained with Sudan IV and the findings quantified (**b**). **c** Representative images of macrophage infiltration; tissue was stained with ER-HR3 and the findings quantified (**d**). Results show decreased plaque burden and macrophage infiltration in KK*Ay*$^{+}$*Apoe*$^{-/-}$*Ccr2*$^{-/-}$ mice compared with KK*Ay*$^{+}$*Apoe*$^{-/-}$ mice. Experiments were repeated three times; n=3–5. *p<0.05

Diabetic nephropathy The metabolic syndrome is a major risk factor for the development of diabetic nephropathy [3]. The pathology of diabetic nephropathy is characterised by mesangial expansion, glomerular basement membrane thickening and nodular sclerosis [27, 28]. Most murine models fail to duplicate the pathological features of diabetic nephropathy (ESM Table 3). In KK*Ay*$^{+}$*Apoe*$^{-/-}$ mice, but not in KK*Ay*$^{+}$ or *Apoe*$^{-/-}$ mice, we observed several histopathological features of diabetic nephropathy (Fig. 3a, b). Inactivation of *Ccr2* seems to afford protection against features of diabetic nephropathy. Mesangial expansion, as indicated by glycogen deposition in the glomeruli, was more prominent in kidneys from KK*Ay*$^{+}$*Apoe*$^{-/-}$ mice than in those from KK*Ay*$^{-}$*Apoe*$^{-/-}$ and KK*Ay*$^{+}$*Apoe*$^{-/-}$*Ccr2*$^{-/-}$ mice (Fig. 3a, b). Electron microscopy revealed thickened basement membrane in KK*Ay*$^{+}$*Apoe*$^{-/-}$ mice compared with KK*Ay*$^{-}$*Apoe*$^{-/-}$ mice (ESM Fig. 2). Nodular sclerosis was present in 20 to 30% of KK*Ay*$^{+}$*Apoe*$^{-/-}$ mice, while KK*Ay*$^{-}$*Apoe*$^{-/-}$ and KK*Ay*$^{+}$*Apoe*$^{-/-}$*Ccr2*$^{-/-}$ mice had no signs of sclerosis (Fig. 3c). The presence of histopathological features of diabetic nephropathy and the protection afforded by the *Ccr2*-null state were further substantiated by decreased collagen deposition (Fig. 3d) and open capillary lumen area (Fig. 3e), even when corrected for glomerular volume (Fig. 3f). Clinically, serum creatinine and the urinary albumin:creatinine ratio were not significantly different among all groups (data not shown), suggesting that a longer follow-up is necessary, or that additional factors (e.g. hypertension, bradykinin, angiotensin) are required to influence renal function.

Potential mechanisms accounting for the protective effects of *Ccr2* inactivation

Accumulation of inflammatory monocytes in epididymal fat pads is thought to contribute to local production of inflammatory cytokines and mediators that promote insulin resistance [29]. We found that the protective effects of *Ccr2* inactivation against insulin resistance in KK*Ay*$^{+}$*Apoe*$^{-/-}$ mice were unlikely to be due to changes in the amount of epididymal fat pads (Table 1) or to have occurred via quantitative changes in inflammatory monocyte content of epididymal fat pads, since the proportion

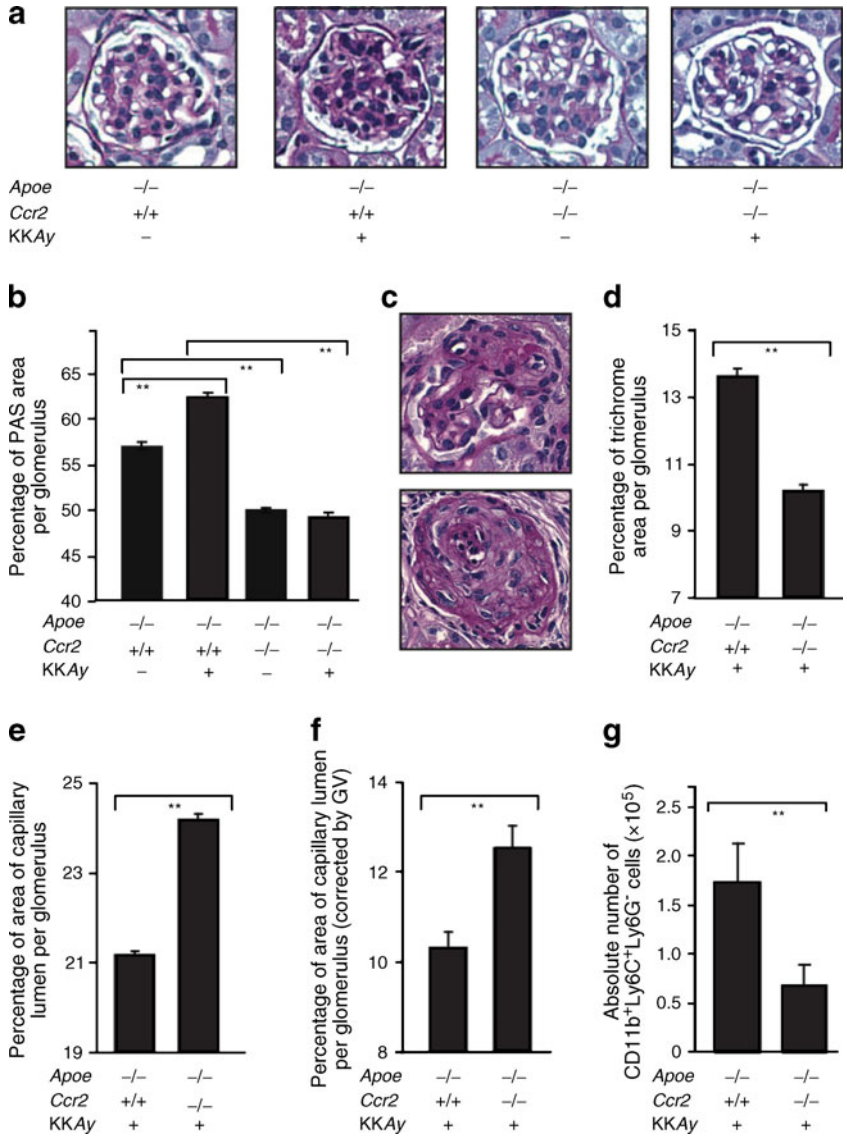

Fig. 3 *Ccr2* inactivation and kidney involvement in the metabolic syndrome. Periodic acid–Schiff's reagent (PAS) staining, shown as histopathological images (**a**) with quantification (**b**), showed glycogen deposition in all four groups of mice (age 25±5 weeks). **c** Staining showed nodular sclerosis to be present only in KK*Ay*$^{+}$*Apoe*$^{-/-}$ mice (two representative stained sections from these mice are shown).**d** Collagen deposition was assessed by Masson's trichrome staining. **e** Percentage of capillary lumen area per glomerulus and (**f**) lumen area corrected by glomerular volume (GV) were calculated as described. In all the cases, 50 to 80 glomeruli were analysed per mouse. **g** The *Ccr2*-null state was associated with less macrophage infiltration in the kidneys. Images and data are representative of three experiments; n=3–5 per group. **p<0.01

of these cells was comparable between KK*Ay*$^{+}$*Apoe*$^{-/-}$ and KK*Ay*$^{+}$*Apoe*$^{-/-}$*Ccr2*$^{-/-}$ mice, even after controlling for body weight (Table 2 and Fig. 4). Likewise, there were no differences in the proportion of inflammatory monocytes in the pancreas (Fig. 4 and Table 2). In contrast, we found a significant reduction in the proportion of inflammatory monocytes in the liver, muscle, kidney and blood of KK*Ay*$^{+}$*Apoe*$^{-/-}$*Ccr2*$^{-/-}$ mice (Figs 3g and 4 and Table 2).

We surmised that differences in the proportion of inflammatory monocytes in organs other than epididymal fat pads could be closely involved in the regulation of glucose metabolism and also contribute to the development of insulin resistance. Indeed, we found that the proportion of inflammatory monocytes in the liver, pancreas and muscle, but not in the epididymal fat pads and blood, were significantly correlated with peripheral glucose levels (Table 3 and ESM Fig. 3). Even after accounting for differences such as age and body weight, these differences remained significant (Table 2). Together the data in Tables 2 and 3 suggest that inactivation of *Ccr2* in KK*Ay*$^{+}$*Apoe*$^{-/-}$ mice may ameliorate insulin resistance via modulation of inflammatory monocyte accumulation, mostly in liver and muscle, but not in the epididymal fat pads.

Lastly, we asked whether absence of CCR2 was associated with changes in the phosphorylation of molecules in the insulin-signalling pathway. Based on several studies in humans documenting that early changes in muscle are associated with insulin resistance [30], we focused on this tissue. In the muscle of KK*Ay*$^{+}$*Apoe*$^{-/-}$ mice, inactivation of *Ccr2* was associated with significantly lower levels of glycogen synthase kinase 3β (GSK-3β) phosphorylation (pGSK-3β), but not of Akt, IGF-1R and p70S6 kinase (ESM Fig. 4 and data not shown). This difference was also

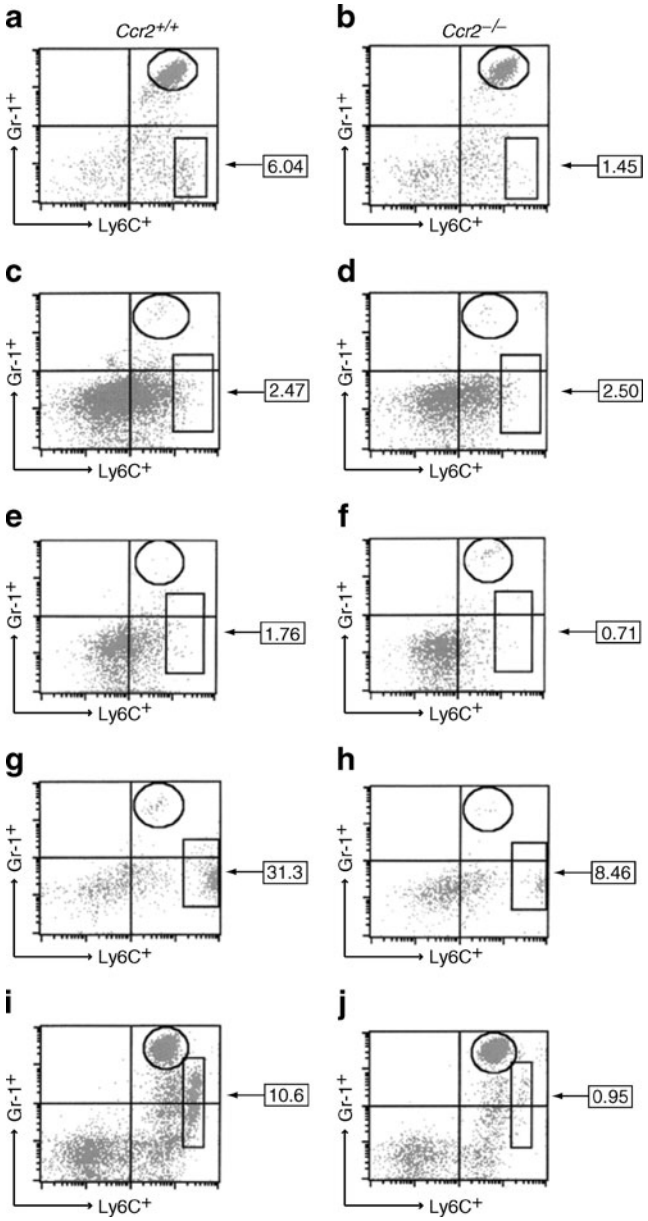

Fig. 4 FACS plots representing the percentage of inflammatory monocytes in different organs of KK*Ay*$^{+}$*Apoe*$^{-/-}$ and KK*Ay*$^{+}$*Apoe*$^{-/-}$*Ccr2*$^{-/-}$ mice. All plots were gated on CD11b^{+} and specific populations for Gr-1 and Ly6C^{+} were selected as shown. Infiltration in liver (**a**, **b**), epididymal fat pads (**c**, **d**), pancreas (**e**, **f**), muscle (**g**, **h**) and blood (**i**, **j**) is shown; n= 9–15 per group

observed in the liver, but not in the epididymal fat pads. Lower levels of pGSK-3β in KK*Ay*$^{+}$*Apoe*$^{-/-}$*Ccr2*$^{-/-}$ muscle tissue remained significant even after controlling for body weight (p=0.005). Remarkably, levels of pGSK-3β in muscle correlated with serum glucose at 120 min post-insulin administration (r=0.85, p=0.014, df=5; partial correlation using body weight and genotype as covariates, n=10). Ingenuity pathways analysis looking for interactions between CCR2 and pGSK-3β in insulin resistance revealed that they could potentially be linked via activation of the transcription factor, signal transducer and activator of transcription 3 (STAT3) (ESM Fig. 5, ESM Methods).

Discussion

Here we generated a model system to capture the complex pathogenesis and clinical manifestations of the metabolic syndrome and its complications. We show that inactivation of *Apoe* in KK*Ay*$^{+}$ mice leads to the development of features that define the metabolic syndrome, such as obesity, insulin resistance and dyslipidaemia, and to complications including atherogenesis and diabetic nephropathy. In this model system, *Ccr2* gene inactivation was associated with a reduction in insulin resistance and weight gain, but dyslipidaemia was not affected. We also found a decrease in plaque burden and observed changes in the kidney normally seen in diabetic nephropathy. The data suggest that a potential mechanism for the protective effects of *Ccr2* inactivation is a reduction in the proportion of inflammatory monocytes in the liver and muscle, but not in the epididymal fat pads.

To our knowledge, other murine models do not display the defining features and complications of the metabolic syndrome that we have described in KK*Ay*$^{+}$*Apoe*$^{-/-}$ mice (ESM Table 1). For example, Gao et al. [31] studied the role of apolipoprotein E in a mouse model of diabetes, for which they backcrossed KK*Ay*$^{+}$ mice with *Apoe*$^{-/-}$, *Apoe*$^{-/+}$ or *Apoe*$^{+/+}$ mice; unfortunately they did not describe in detail cardiovascular complications, i.e. atherosclerosis.

We chose KK*Ay*$^{+}$ mice because, similarly to humans, the development of the metabolic complications in this system is polygenic [13]. Genetic inactivation of *Apoe* in these mice was important because C57BL/6J wild-type mice on a HFD [32] only developed a mild form of insulin resistance and dyslipidaemia, with almost undetectable plaques and minimal diabetic nephropathy [33]. Likewise, type 2 diabetes-prone KK*Ay*$^{+}$ mice on a HFD followed by LPS injections as administered here do not develop significant atherosclerosis. *Apoe*$^{-/-}$ mice, a well-known murine model classically used for the study of dyslipidaemia-induced

Table 3 Correlation between inflammatory monocytes and glucose levels

Organ	Correlation	p value
Liver	0.42	0.041
Epididymal fat pads	–	NS
Pancreas	0.58	0.029
Muscle	0.55	0.006
Blood	–	NS

Analysis includes the use of age, sex and body weight as covariates; n=30

atherosclerosis, do not develop insulin resistance and, even on a HFD, the defining features of the metabolic syndrome tend to be mild [34].

The work shown here provides further support for the notion that CCR2 plays a critical role in the metabolic syndrome, but also reveals potentially new pathogenic effects. It has been postulated that, in the context of obesity, CCR2–CCL2-dependent monocyte recruitment into adipose tissue promotes local inflammation and impairment of adipocyte function [35]. Adipocytes and inflammatory monocyte-derived macrophages in the epididymal fat pads produce pro-inflammatory cytokines such as IL-6 and TNFα, which can induce insulin resistance [10]. Administration of propagermanium for pharmacological blockade of CCR2 in mice reduced adipose tissue inflammation and the related insulin resistance [36]. Our data also support the notion that defective macrophage migration induced by modulation of the *Ccr2–Ccl2* axis may play a major role in atherosclerosis and diabetic nephropathy.

Unlike previous reports using less complex diet-based models [9], our work indicates that CCR2 may contribute to the pathogenesis of the metabolic syndrome via its effects on accumulation of inflammatory monocytes in the muscle and liver, but not in the epididymal fat pads. The precise mechanism responsible for CCR2-driven accumulation of inflammatory monocytes in liver and muscle, which might result in insulin resistance, remains to be explored. A reasonable hypothesis is that infiltrating inflammatory monocytes produce inflammatory mediators that affect local responses to insulin in the liver and muscle. In support of this concept, our results showed decreased phosphorylation of GSK-3β in muscle and liver of *Ccr2*-knockout mice. GSK-3β regulates insulin action and glucose metabolism in human skeletal muscle [37]. In the kidney [38], GSK-3β has been shown to regulate glucose- and insulin-induced extracellular matrix production in renal proximal tubular cells. In the arterial wall, GSK-3β modulates the development of atherosclerosis [39]. Pathway analysis (ESM Fig. 5, ESM Methods) suggested that STAT3 could act as a link between CCR2 and GSK-3β in the development of insulin resistance. Future studies will need to directly explore the mechanisms underlying the effects of tissue-specific inflammatory monocyte infiltration on insulin signalling and glucose uptake, for example by using radioactive tracers and insulin clamp processes.

Our finding that KK$Ay^{+}Apoe^{-/-}$ and KK$Ay^{+}Apoe^{-/-}Ccr2^{-/-}$ mice had similar food intake revealed that *Ccr2* inactivation does not affect the satiety regulation pathways that are disrupted in mice with the Ay^{+} allele (ESM Methods). This finding contrasts with the observation of Weisberg et al. [9] that inactivation of *Ccr2* in mice on a HFD reduces food intake. This discrepancy may be due to the fact that our mice were fed a normal diet and became obese due to hyperphagia.

We characterised two complications of the metabolic syndrome, namely atherosclerosis and diabetic nephropathy. KKAy^{+} mice, even when fed a HFD, develop minimal or no atherosclerotic plaque lesions, and only minor morphological renal abnormalities (data not shown). $Apoe^{-/-}$ mice normally develop hypercholesterolaemia and atherosclerosis [14], but do not have prominent kidney abnormalities (ESM Table 3). In our studies, KK$Ay^{+}Apoe^{-/-}$ mice were characterised by severe and accelerated atherosclerotic plaque burden (1–2 log increase in plaque size compared with $Apoe^{-/-}$ mice), and by kidney changes indicative of diabetic nephropathy, e.g. marked glycogen and collagen deposition in the glomeruli, as well as glomerulosclerosis (20% of mice), all in the context of macrophage infiltration.

In our studies, we did not find any differences in the albumin:creatinine ratio from 24 h urine samples in KK$Ay^{+}Apoe^{-/-}$ mice, indicating that, over the time period studied, only the histological changes, but not clinical manifestations of diabetic nephropathy were present. The inability to recreate hypertension in our model system may have prevented the emergence of full-blown diabetic nephropathy. Future experiments will need a longer follow-up in order to determine whether KK$Ay^{+}Apoe^{-/-}$ mice develop hypertension and proteinuria at later time points. In any case, factors affecting proteinuria or loss of renal function may be different from those affecting mesangial expansion and fibrosis, implying that multiple pathways are involved in the development of diabetic nephropathy [40].

Collectively our findings highlight the usefulness of a novel murine model for dissecting the pathogenesis of the metabolic syndrome. In this model system, we found that CCR2 plays a critical role. This finding suggests that modulation of the chemokines axis could be a relevant approach for therapy of the defining features and complications of the metabolic syndrome.

Acknowledgements We thank Y. Patel (Department of Pathology, UTHSCSA) for help with HPLC measurement of creatinine. This work was supported by grants from Fraternal Order of Eagles, a Veterans' Administration Merit Award, and NIH RO1 AR 052755 to S. S. Ahuja.

Contribution statement All authors were involved in conception and design, analysis and interpretation of data, drafting or revision, and final approval of the article to be published.

Duality of interest The authors declare that there is no duality of interest associated with this manuscript.

References

1. Ford ES, Giles WH, Dietz WH (2002) Prevalence of the metabolic syndrome among US adults: findings from the third National Health and Nutrition Examination Survey. JAMA 287:356–359
2. Haffner SM (2006) The metabolic syndrome: inflammation, diabetes mellitus, and cardiovascular disease. Am J Cardiol 97:3A–11A
3. Hayden MR, Whaley-Connell A, Sowers JR (2005) Renal redox stress and remodeling in metabolic syndrome, type 2 diabetes mellitus, and diabetic nephropathy: paying homage to the podocyte. Am J Nephrol 25:553–569
4. Stewart JH, McCredie MR, Williams SM, Jager KJ, Trpeski L, McDonald SP (2007) Trends in incidence of treated end-stage renal disease, overall and by primary renal disease, in persons aged 20–64 years in Europe, Canada and the Asia-Pacific region, 1998–2002. Nephrology (Carlton) 12:520–527
5. Penno G, Miccoli R, Pucci L, del Prato S (2006) The metabolic syndrome. Beyond the insulin resistance syndrome. Pharmacol Res 53:457–468
6. Charo IF, Ransohoff RM (2006) The many roles of chemokines and chemokine receptors in inflammation. N Engl J Med 354:610–621
7. Boring L, Gosling J, Chensue SW et al (1997) Impaired monocyte migration and reduced type 1 (Th1) cytokine responses in C-C chemokine receptor 2 knockout mice. J Clin Invest 100:2552–2561
8. Sato N, Ahuja SK, Quinones M et al (2000) CC chemokine receptor (CCR)2 is required for Langerhans cell migration and localization of T helper cell type 1 (Th1)-inducing dendritic cells. Absence of CCR2 shifts the *Leishmania major*-resistant phenotype to a susceptible state dominated by Th2 cytokines, B cell outgrowth, and sustained neutrophilic inflammation. J Exp Med 192:205–218
9. Weisberg SP, Hunter D, Huber R et al (2006) CCR2 modulates inflammatory and metabolic effects of high-fat feeding. J Clin Invest 116:115–124
10. Weisberg SP, McCann D, Desai M, Rosenbaum M, Leibel RL, Ferrante AW Jr (2003) Obesity is associated with macrophage accumulation in adipose tissue. J Clin Invest 112:1796–1808
11. Barlic J, Murphy PM (2007) Chemokine regulation of atherosclerosis. J Leukoc Biol 82:226–236
12. Galkina E (2006) Leukocyte recruitment and vascular injury in diabetic nephropathy. J Am Soc Nephrol 17:368–377
13. Suto J, Matsuura S, Imamura K, Yamanaka H, Sekikawa K (1998) Genetics of obesity in KK mouse and effects of A(y) allele on quantitative regulation. Mamm Genome 9:506–510
14. Zhang SH, Reddick RL, Piedrahita JA, Maeda N (1992) Spontaneous hypercholesterolemia and arterial lesions in mice lacking apolipoprotein E. Science 258:468–471
15. Kuziel WA, Dawson TC, Quinones M et al (2003) CCR5 deficiency is not protective in the early stages of atherogenesis in apoE knockout mice. Atherosclerosis 167:25–32
16. Kuziel WA, Morgan SJ, Dawson TC et al (1997) Severe reduction in leukocyte adhesion and monocyte extravasation in mice deficient in CC chemokine receptor 2. Proc Natl Acad Sci U S A 94:12053–12058
17. Dawson TC, Kuziel WA, Osahar TA, Maeda N (1999) Absence of CC chemokine receptor-2 reduces atherosclerosis in apolipoprotein E-deficient mice. Atherosclerosis 143:205–211
18. Quinones MP, Martinez HG, Jimenez F et al (2007) CC chemokine receptor 5 influences late-stage atherosclerosis. Atherosclerosis 195:e92–e103
19. Pagtalunan ME, Rasch R, Rennke HG, Meyer TW (1995) Morphometric analysis of effects of angiotensin II on glomerular structure in rats. Am J Physiol 268:F82–F88
20. Soos TJ, Sims TN, Barisoni L et al (2006) CX3CR1^{+} interstitial dendritic cells form a contiguous network throughout the entire kidney. Kidney Int 70:591–596
21. Iwatsuka H, Shino A, Suzuoki Z (1970) General survey of diabetic features of yellow KK mice. Endocrinol Jpn 17:23–35
22. Srivastava RA (2009) Fenofibrate ameliorates diabetic and dyslipidemic profiles in KKAy mice partly via down-regulation of 11beta-HSD1, PEPCK and DGAT2. Comparison of PPARalpha, PPARgamma, and liver x receptor agonists. Eur J Pharmacol 607:258–263
23. Ohashi K, Kihara S, Ouchi N et al (2006) Adiponectin replenishment ameliorates obesity-related hypertension. Hypertension 47:1108–1116
24. Mark AL, Shaffer RA, Correia ML, Morgan DA, Sigmund CD, Haynes WG (1999) Contrasting blood pressure effects of obesity in leptin-deficient *ob*/*ob* mice and agouti yellow obese mice. J Hypertens 17:1949–1953
25. Koster A, Stenholm S, Alley DE et al (2010) Body fat distribution and inflammation among obese older adults with and without metabolic syndrome. Obesity (Silver Spring) 18:2354–2361
26. Ford ES (2005) Risks for all-cause mortality, cardiovascular disease, and diabetes associated with the metabolic syndrome: a summary of the evidence. Diabetes Care 28:1769–1778
27. Deak G (1976) Nodular thickening of peritubular basement membranes in diabetic kidneys. Acta Morphol Acad Sci Hung 24:191–202
28. Olsen S (1972) Mesangial thickening and nodular glomerular sclerosis in diabetes mellitus and other diseases. Acta Pathol Microbiol Scand Suppl 233:203–216
29. Permana PA, Menge C, Reaven PD (2006) Macrophage-secreted factors induce adipocyte inflammation and insulin resistance. Biochem Biophys Res Commun 341:507–514
30. St-Pierre P, Genders AJ, Keske MA, Richards SM, Rattigan S (2010) Loss of insulin-mediated microvascular perfusion in skeletal muscle is associated with the development of insulin resistance. Diabetes Obes Metab 12:798–805
31. Gao J, Katagiri H, Ishigaki Y et al (2007) Involvement of apolipoprotein E in excess fat accumulation and insulin resistance. Diabetes 56:24–33
32. van Weel V, de Vries M, Voshol PJ et al (2006) Hypercholesterolemia reduces collateral artery growth more dominantly than hyperglycemia or insulin resistance in mice. Arterioscler Thromb Vasc Biol 26:1383–1390
33. Rodriguez WE, Tyagi N, Joshua IG et al (2006) Pioglitazone mitigates renal glomerular vascular changes in high-fat, high-calorie-induced type 2 diabetes mellitus. Am J Physiol Renal Physiol 291:F694–F701
34. Lohmann C, Schafer N, von Lukowicz T et al (2009) Atherosclerotic mice exhibit systemic inflammation in periadventitial and visceral adipose tissue, liver, and pancreatic islets. Atherosclerosis 207:360–367
35. Kanda H, Tateya S, Tamori Y et al (2006) MCP-1 contributes to macrophage infiltration into adipose tissue, insulin resistance, and hepatic steatosis in obesity. J Clin Invest 116:1494–1505
36. Tamura Y, Sugimoto M, Murayama T et al (2008) Inhibition of CCR2 ameliorates insulin resistance and hepatic steatosis in *db*/*db* mice. Arterioscler Thromb Vasc Biol 28:2195–2201
37. Nikoulina SE, Ciaraldi TP, Mudaliar S, Carter L, Johnson K, Henry RR (2002) Inhibition of glycogen synthase kinase 3 improves insulin action and glucose metabolism in human skeletal muscle. Diabetes 51:2190–2198
38. Mariappan MM, Shetty M, Sataranatarajan K, Choudhury GG, Kasinath BS (2008) Glycogen synthase kinase 3beta is a novel regulator of high glucose- and high insulin-induced extracellular matrix protein synthesis in renal proximal tubular epithelial cells. J Biol Chem 283:30566–30575
39. Robertson LA, Kim AJ, Werstuck GH (2006) Mechanisms linking diabetes mellitus to the development of atherosclerosis: a role for endoplasmic reticulum stress and glycogen synthase kinase-3. Can J Physiol Pharmacol 84:39–48
40. Karalliedde J, Viberti G (2010) Proteinuria in diabetes: bystander or pathway to cardiorenal disease? J Am Soc Nephrol 21:2020–2027